Optimal Dispatch Based on Prediction of Distributed Electric Heating Storages in Combined Electricity and Heat Networks

Haixin Wang[1], Junyou Yang[1*], Zhe Chen[2], Gen Li[3], Jun Liang[3], Yiming Ma[1], Henan Dong[4], Huichao Ji[1] and Jiawei Feng[1]
(1. Shenyang University of Technology, Shenyang, 110870, China 2. Aalborg University, Aalborg, 9220, Denmark
3. Cardiff University, Cardiff, CF24 3AA, UK 4. Electric Power Research Institute of State Grid Liaoning Electric Power Supply Co. Ltd., Shenyang, 110006, China)

***Abstract*—The volatility of wind power generations could significantly challenge the economic and secure operation of combined electricity and heat networks. To tackle this challenge, this paper proposes a framework of optimal dispatch with distributed electric heating storage based on a correlation-based long short-term memory prediction model. The prediction model of distributed electric heating storage is developed to model its behavior characteristics which are obtained by the auto-correlation and correlation analysis with external factors including weather and time-of-use price. An optimal dispatch model of combined electricity and heat networks is then formulated and resolved by a constraint reduction technique with clustering and classification. Our method is verified through numerous simulations. The results show that, compared with the state-of-the-art techniques of support vector machine and recurrent neural networks, the mean absolute percentage error with the proposed correlation-based long short-term memory can be reduced by 1.009 and 0.481 respectively. Compared with conventional method, the peak wind power curtailment with dispatching distributed electric heating storage is reduced by nearly 30% and 50% in two cases respectively.**

***Index Terms*—Power system, combined electricity and heat networks, distributed electric heating storage, demand response, optimal dispatch.**

I. Introduction

With the increase of renewable energy integration and load, electricity and heat of multi-energy systems are coupled, which challenges the optimal dispatch and secure operation of the combined electricity and heat networks (CEHN). For instance, the curtailment of wind power in Northern China will become more severe in winter due to the significant thermal requirements supplied by combined heat and power (CHP) units [1,2]. It is urgent to tackle the wind power curtailment and energy optimization.

Demand response (DR) has been widely recognized as an effective approach to achieve energy optimization in CEHN by shifting loads from high-peak to off-peak hours [3-5]. According to the DR's operation characteristics, there are mainly four types of DR as follows: ***1)*** Flexible electric loads; These loads are scheduled based on electricity price and incentives [6]; ***2)*** Electric energy storage (EES) [7]. EES helps fill the valleys and shave the peaks of the demand profiles. However, the costs and geographical characteristics (e.g. flywheel and pumped storage) are still their main limitations; ***3)*** Heat loads [8]. Thanks to their thermal inertia, heat loads can help regulate CHP within a certain period [9]; ***4)*** Thermal energy storage (TES) [10]. CHP's regulation capability can be enhanced if TES is deployed in a CHP [11].

The above DRs have been widely applied to district heating networks. However, a distributed heating network, which has the advantages of flexible control and operation, has been rarely considered in the dispatch of CEHN. This paper develops a new DR using distributed electric heating storage (DEHS) in distributed heating networks for the optimal dispatch of CEHN. Compared with the above DRs, DEHS has the following characteristics which have also been indicated in the previous works such as [12] and [13]. ***a)*** DEHS operates as both an electric load and a heat source. ***b)*** The generated thermal power is stored by special insulation bricks so that it can store as well as release thermal power simultaneously. ***c)*** DEHS operates mainly in winter, and its operation power curve is related to the peak and valley electricity price and weather factors. ***d)*** Individual DEHS operates mainly at nominal electric power. DEHS can offer large amounts of thermal storage capacity without massive investments [12]. Based on the above analysis, DEHS can be considered as an excellent choice to provide additional flexibility to the CEHN. The electric heating storage system has been studied in [13]. However, its focus is the performance of the device without the consideration of prediction and optimal dispatch in CEHN.

In methods of DR prediction, the prediction error in the optimal dispatch is usually represented by random variables in some probability distributions (e.g. Gaussian or Beta) [14]. However, it cannot give the accurate statistical characterization of such random variables for some special loads [15]. The commonly used short-time load prediction approach is to make a certain reasoning or guessing about its future trend based on the analysis of historical power data, such as regression analysis and time series methods [16,17]. Short-term load prediction that depends on customer behaviors, events, and environmental factors may induce a high degree of uncertainty. The accuracy of these short-term forecasting techniques might become degraded dramatically [18,19].

Deep neural networks have been recently presented, which are promising architectures to provide comprehensive and detailed information from raw data, such as multi-layer neural network, deep belief neural network, recurrent neural network

* Corresponding Author: Junyou Yang
Email: junyouyang@sut.edu.cn

(RNN) and support vector machine (SVM) [20]. Among them, long short-term memory (LSTM) is considered as an effective method to tackle the time series forecasting challenges owing to its efficient performance for accurate modeling of complex nonlinear time-dependent parameters [21-23]. There are a few interesting works which have developed LSTM based techniques for modeling residential load in power system. Reference [24] explores an LSTM recurrent neural network to identify active power fluctuations in real-time. To recognize industrial equipment in manufacturing systems, an LSTM is adopted to analyze big data features [25]. An LSTM recurrent neural network-based framework is proposed to predict aggregated residential load on a large scale [26]. In particular, weather data (such as temperature, wind speed, cloud cover, etc) are considered to enhance the accuracy of LSTM based power load prediction [27]. However, due to the sudden changes in the electric power curve of DEHS caused by the time-of-use price, only considering weather factor is not sufficient to achieve an accurate prediction. Besides, oversimplifying the uncertainties on the demand side may fail to reflect the real state of distributed heating networks (DHNs). The prediction model is influenced by behavior characteristics integrating sequence characteristics, time-of-use price and distributed heat load (DHL) requirements related to weather. Therefore, it is necessary to develop a new LSTM model for DEHS considering those factors. Our contributions are as follows.

- To the best of our knowledge, this is the first work for scheduling the DEHS with the proposed framework of optimal dispatch based on a prediction model to enhance wind power accommodation and system stability.
- A correlation-based (C-LSTM) prediction model framework of DEHS, considering behavior characteristics integrating sequence characteristic and external factors (including weather factors and time-of-use price) is proposed to enhance prediction precision.
- A constraint reduction technique of DHNs model is developed to resolve the difficulty of an optimization problem with large constraints of distributed electric heating networks.
- Compared with the state-of-the-art techniques of SVM and RNN, the mean absolute percentage error (MAPE) with the proposed C-LSTM can be reduced by 1.009 and 0.481 respectively. Compared with no dispatching DEHS, the peak wind power with dispatching DEHS curtailment is reduced by nearly 30% and 50% in two cases respectively.

II. PRELIMINARIES

A. Overall Structure

The overall schematic diagram of CEHN is shown in Fig. 1. The electric network is composed of CHP, thermal power plant (TPP), wind power plant (WPP), EES, DEHS and electric loads. The district heating network includes CHP, TES and heat loads. Moreover, each distributed heating network consists of DEHS and DHL. It can be seen that electric network, district heating network and distributed heating networks interact with each other.

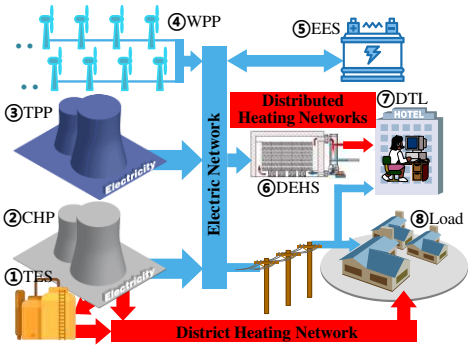

Fig. 1 Schematic diagram of combined electricity and heat networks.

B. Operation Constraints and Costs

(1) CHP with TES

a) Analysis of operation characteristics

In the heating season, CHP is used as the main electric power source to guarantee consumers' thermal requirements. TES can absorb heat from CHP and release heat to the district heating network simultaneously. As shown in Fig. 2, $P^{\mathrm{E}}_{CHP,\min}$ and $P^{\mathrm{E}}_{CHP,\max}$ are the minimum and maximum electric power of the CHP without thermal power production. $P^{\mathrm{T}}_{CHP,\max}$ and $P^{\mathrm{T}}_{TES,\max}$ are the maximum thermal power of the CHP and TES. Hereafter, the subscripts 'max' and 'min' indicate the maximum and minimum of variables. The operation region of the CHP is within the area of A-B-C-D as shown in Fig. 2. The coupling characteristic of CHP may lead to electric network instability. For example, the electric power output of CHP will be added with the increase of thermal requirement. The regulation range of electric power will be narrowed. The wind power curtailment may be induced if the wind power penetration of electric network is increased. The operation region can be expanded to the area of A-E-F-G-H-I if the TES is deployed with the CHP. The thermoelectric couple of CHP is reduced. The following models and equations can be found in [1,8,11]. We include them here for the completeness.

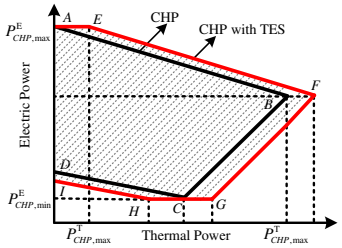

Fig. 2. Thermal-electricity relationship of the CHP with TES.

b) Constraints of CHP and TES

According to the operation characteristics of CHP, the constraints of electric power $P^{\mathrm{E}}_{CHPi,t}$ and thermal power $P^{\mathrm{T}}_{CHPi,t}$ for CHP$_i$ (i=1, …, I, and I is the total number of CHP) at time t (t=1, …, T, and T is the total time points) are given by (1).

$$\begin{cases} (P^{\mathrm{E}}_{CHPi,\min} - c_v P^{\mathrm{T}}_{CHPi,t}) \le P^{\mathrm{E}}_{CHPi,t} \le (P^{\mathrm{E}}_{CHPi,\max} - c_v P^{\mathrm{T}}_{CHPi,t}) \\ R^{\mathrm{E}}_{CHPi,\min} \le P^{\mathrm{E}}_{CHPi,t} - P^{\mathrm{E}}_{CHPi,t-1} \le R^{\mathrm{E}}_{CHPi,\max} \\ P^{\mathrm{T}}_{CHPi,\min} \le P^{\mathrm{T}}_{CHPi,t} \le P^{\mathrm{T}}_{CHPi,\max} \end{cases}, \quad (1)$$

where c_v is the conversion coefficient from thermal power to electric power, $R^{\mathrm{E}}_{CHPi,\min}$ and $R^{\mathrm{E}}_{CHPi,\max}$ are the lower and upper ramp rate limits of CHP i respectively.

The constraints of thermal power $P^{\mathrm{T}}_{TESj,t}$ and capacity $S^{\mathrm{T}}_{TESj,t}$ for TES$_j$ (j=1, …, J, and J is the total number of TES) are expressed by (2).

$$\begin{cases} P^{\mathrm{T}}_{TESj,\min} \le P^{\mathrm{T}}_{TESj,t} \le P^{\mathrm{T}}_{TESj,\max} \\ S^{\mathrm{T}}_{TESj,\min} \le (S^{\mathrm{T}}_{TESj,t} = S^{\mathrm{T}}_{TESj,t-1} + P^{\mathrm{T}}_{TESj,t} - P^{\mathrm{T}}_{TESj,out,t}) \le S^{\mathrm{T}}_{TESj,\max} \end{cases}, \quad (2)$$

where $P^{\mathrm{T}}_{TESj,out,t}$ is the output thermal power of TES$_j$.

c) Cost of CHP with TES

The operation cost of CHP with TES C_{CT} is described in (3).

$$\begin{cases} C_{CT} = \sum_{i=1}^{I} C_{CHPi} + \sum_{j=1}^{J} C_{TESj} \\ C_{CHPi} = \sum_{t=1}^{T} \{ a_i \left[P^{\mathrm{E}}_{CHPi,t} + c_v P^{\mathrm{T}}_{CHPi,t} \right]^2 + b_i \left[P^{\mathrm{E}}_{CHPi,t} + c_v P^{\mathrm{T}}_{CHPi,t} \right] + c_i \}, \\ C_{TESj} = \sum_{t=1}^{T} (c_{o1} P^{T}_{TESj,t}) \end{cases} \quad (3)$$

where C_{CHPi} is the fuel cost of CHP$_i$, C_{TESj} is the operation and maintenance cost of TES$_j$, a_i, b_i and c_i are the operation cost coefficients, c_{o1} is the operation cost coefficient.

(2) Thermal Power Plant

In the heating season, TPP can assist the CHP to regulate the power variation of the electric network. The interested reader can refer to [28] for more details about constraints and additional formulations which represent minimum up/downtimes or startup and shutdown trajectories for each TPP. The output of the TPP is limited by the minimum load, maximum capacity and ramp rates. The operation constraints of electric power $P_{TPPk,t}$ for TPP$_k$ (k=1, …, K, and K is the total number of TPP) at time t are described in (4).

$$\begin{cases} P_{TPPk,\min} \le P_{TPPk,t} \le P_{TPPk,\max} \\ R_{TPPk,\min} \le P_{TPPk,t} - P_{TPPk,t-1} \le R_{TPPk,\max} \end{cases}, \quad (4)$$

where $R_{TPPk,\min}$ and $R_{TPPk,\max}$ are the lower and upper ramp rate limits. The fuel cost C_{TPP} can be obtained by (5).

$$C_{TPP} = \sum_{k=1}^{K} \sum_{t=1}^{T} (a_k P_{TPPk,t}{}^2 + b_k P_{TPPk,t} + c_k), \quad (5)$$

where a_k, b_k and c_k are the cost coefficients of TPP$_k$.

(3) Wind Power Plant

To simplify the analysis, the average value of wind speed (v_a) is used to calculate the wind power $P_{WPPm,t}$ in (6).

$$P_{WPPm,t} = \begin{cases} 0, & 0 \le v_a < v_r \\ P_{WPPm,rated} \times \dfrac{v_a - v_{ci}}{v_r - v_{ci}}, & v_{ci} \le v_a < v_r \\ P_{WPPm,rated}, & v_{ci} \le v_a < v_{co} \\ 0, & v_{co} \le v_a \end{cases}, \quad (6)$$

where $P_{WPPm,rated}$ is the rated output power of WPP$_m$ (m=1, …, M, and M is the total number of WPP), v_{ci}, v_r and v_{co} are the cut-in speed, rated speed and cut-off speed of the wind turbine, respectively.

The cost of wind power curtailment C_W is described in (7).

$$C_W = c_Q \sum_{m=1}^{M} \sum_{t=1}^{T} \Delta P_{WPPm,t}, \quad (7)$$

where c_Q is the cost coefficient of wind power curtailment. $\Delta P_{WPPm,t}$ is wind power curtailment of WPP$_m$.

(4) Electric Energy Storage

EES will be charged during load valley periods and discharged during load peak periods. In this way, EES can effectively reduce the different values between peak and valley and therefore, improve the stability of the electric network. However, EES with large capacity will increase the economic cost of electric network. EES will stop charging and discharging when it reaches the maximum and minimum storage capacity of the battery. The constraints of electric power $P_{EESr,t}$ and capacity $S_{EESr,t}$ for EES$_r$ (r=1, …, R, and R is the number of EES) are given in (8).

$$\begin{cases} P^{c}_{EESr,\max} \le P_{EESr,t} \le P^{d}_{EESr,\max} \\ S_{EESr,t} = S_{EESr,t-1} + P_{EESr,t}(1+\rho^{c}_{EESr}), \text{ when charge} \\ S_{EESr,t} = S_{EESr,t-1} + P_{EESr,t}(1+\rho^{d}_{EESr}), \text{ when discharge} \\ S_{EESr,\min} \le S_{EESr,t} \le S_{EESr,\max} \end{cases}, \quad (8)$$

where $P^{c}_{EESr,\max}$ and $P^{d}_{EESr,\max}$ are the maximum charge and discharge power, ρ^{c}_{EESr} and ρ^{d}_{EESr} are charge and discharge losses of EES$_r$, respectively. The operation cost of EES CEES is calculated by (9).

$$C_{EES} = \sum_{r=1}^{R} \sum_{t=1}^{T} (c_{o2} P_{EESr,t}), \quad (9)$$

where c_{o2} is the operation cost coefficient of EES.

III. Operation Characteristic of DEHS

A. Operation Characteristic

DEHS is built to heat for individual DHL as shown in Fig. 3. The resistance wires are used as the heater, and insulating bricks are applied as the regenerator. Cold steam is heated to hot steam through the heater. Furthermore, cold water is heated to hot water to meet consumer's demand by the heat exchanger.

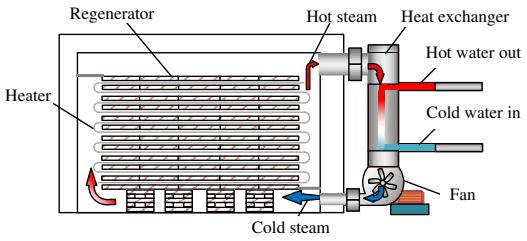

Fig. 3. Structure diagram of DEHS.

The DEHS generally operates at rated power. The basic operation rules of DEHS are as shown in Fig. 4. The DEHS can heat and store in a valley-time price region owing to its cost. The DEHS will switch off the electric power source in a peak-time price region. It will quit operation when the temperature of DEHS is approaching to the limitation, and start again to compensate heat energy before the end of valley time.

TABLE I
AUTO-CORRELATION COEFFICIENT ANALYSIS RESULTS

Lag	Correlation	Lag	Correlation	Lag	Correlation
t-1	0.98	*t*-2	0.95	*t*-3	0.91
t-4	0.87	*t*-5	0.81	*t*-6	0.75
t-7	0.69	*t*-8	0.63	*t*-9	0.57
t-10	0.50	*t*-11	0.44	*t*-12	0.38
t-13	0.32	*t*-14	0.26	*t*-15	0.20

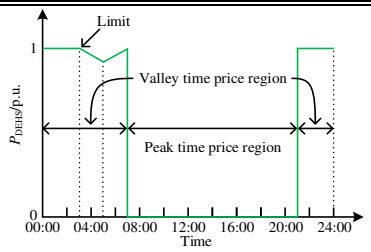

Fig. 4. Operation principle diagram of DEHS.

The operation cost of DEHS C_{DEHS} can be obtained in (10).

$$C_{DEHS} = \sum_{n}^{N}\sum_{t=1}^{T}(c_{o3}\Delta P^{E}_{DEHSn,t}), \tag{10}$$

where $\Delta P^{E}_{DEHSn,t}$ is adjustment power of DEHS$_n$ (n=1, …, N, and N is the number of DEHS) at time t, c_{o3} is the operation cost coefficient of DEHS.

B. Auto-correlation Analysis

To analyze the sequence correlation, the auto-correlation coefficients between original data and different time series are calculated by the Pearson correlation coefficient method in (11).

$$\hat{\rho}_{U,V} = \sum_{l=1}^{L}(u_l-\bar{u})(v_l-\bar{v}) \Big/ \sqrt{\sum_{l=1}^{L}(u_l-\bar{u})^2(v_l-\bar{v})^2}, \tag{11}$$

where $\bar{u}$ and $\bar{v}$ are the empirical means of the samples U=(u_1, …, u_L) and V=(v_1, …, v_L). In this case, U and V represent original power data (U) and lag power data [V=(u_{1+k}, …, u_{L+k}), k is the lag time, k=1, 2, …, i.e., t-k denotes the lag data falls behind the original data by k data points], respectively. The results are shown in Fig. 5 and Table I. Partial autocorrelogram is an important tool to determine the order of autoregressive models for time series. Actually, when it is used to forecast the DEHS power time series, the learning procedure of prediction model is equivalent to building an autoregressive model. Thus, the partial autocorrelograms are utilized to help identify the lag time. According to the partial autocorrelogram, the lag time is selected as 5 [29].

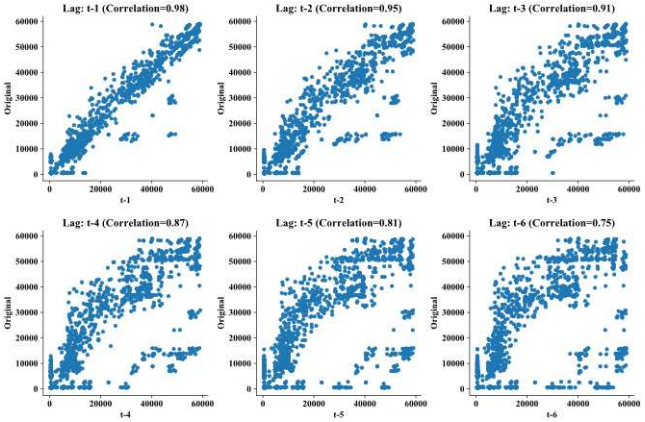

Fig. 5. Auto-correlation coefficients of the electric power data of DEHS.

In Fig. 5, the correlation coefficients are relatively high, which denotes that the history data influence the current data or future data. In Table I, the correlation coefficients would be decreased with the increasing lag time. The electric power data of DEHS have a sequence characteristic, which is suitable for the LSTM model.

C. Correlation Analysis with External Factors

A factor affecting the electric power consumption of DEHS is weather. For example, the weather is cold in winter of Northern China and therefore, the user's heat demand and electric power of DEHS are increased. The consumption of DEHS is also influenced by the time-of-use price for the costs. Therefore, to improve the accuracy of the power prediction, the factors of weather and price are considered. The relationships of power with external factors (including temperature, pressure, humidity, wind speed and time-of-use price) are shown by the scatter plot in Fig. 6. The correlation of electric power with the external factors is calculated based on the Pearson correlation coefficient method in (11). In this case, U and V represent power data and external factors data, respectively. The calculation results are shown in Fig. 7.

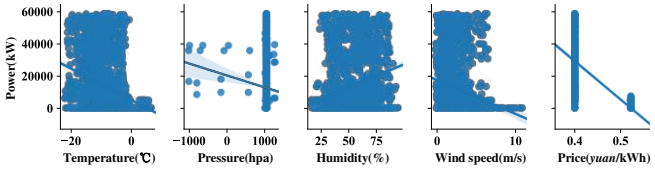

Fig. 6. Scatter plot of power data of DEHS and external factors data.

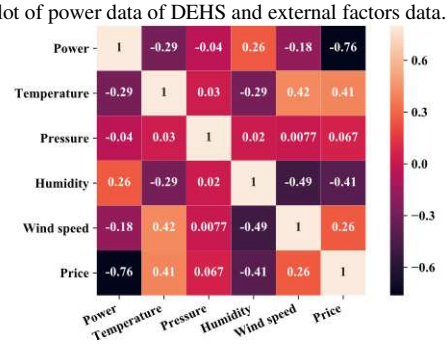

Fig. 7. Correlation coefficients of DEHS with external factors.

In Fig. 7, the correlation coefficients take values between -1 and 1. The closer to 1 the absolute value is, the stronger linear relationship between electric power and external factors is. The sign of coefficients indicates that if the two variables increase or decrease in the same direction (positive) or opposite direction (negative).

IV. OPTIMAL DISPATCH BASED ON PREDICTION OF DEHS

With the increasing penetration of wind power, the wind power curtailment may be induced by a couple of electric and thermal power in CEHN. If the controllable DEHS participates in power balance, the power regulation capability will be enhanced.

In the proposed framework, we develop a prediction model with C-LSTM for DEHSs. Based on the prediction results, a dispatch model is constructed. A reduction technique of DHNs model constraints is then proposed to resolve the difficulty of an optimization problem with large constraints of DHNs. Finally, Sequential Least Squares Programming method is used to optimize the objective function.

A. *Prediction Model Based on C-LSTM*

According to the above analysis, we establish the prediction models for individual DEHS. The essential of RNN is to utilize the sequence characteristics to establish a model, which is suitable for the prediction of DEHS. However, the memory ability of RNN is short-lived, where the context may be significant or useless. As a popular extended RNN method, with three gates (input, forget and output gates) in memory cells, LSTM network can remember, update and focus on effective information, which is helpful to track information for a longer period. LSTM has the advantage of avoiding gradients vanishment and filtering effective information [23]. Each cell is updated based on the current input and the previous cell state. Let c_t be memory cell state at time step t and h_t be the output hidden state, then c_t and h_t are updated by (12).

$$\begin{cases} i_t = \sigma(w_{xi}x_t + w_{hi}x_t + b_i) \\ f_t = \sigma(w_{xf}x_t + w_{hf}x_t + b_f) \\ o_t = \sigma(w_{xo}x_t + w_{ho}x_t + b_o) \\ c_t = f_t \odot c_{t-1} + i_t \odot f(w_{xc}x_t + w_{hc}x_t + b_c) \\ h_t = o_t f(c_t) \end{cases}, \tag{12}$$

where $\sigma(x)=1/(1+e^{-x})$ is the sigmoid function, $f(\cdot)$ is activation function, i_t, f_t and o_t are input gate, forget gate and output gate vectors, w_{xi}, w_{xf}, w_{xo}, w_{hi}, w_{hf} and w_{ho} are the weights for linear combination, b_i, b_f and b_o are the relative bias, and $\odot$ is element-wise production.

In this paper, we consider the behavior characteristics integrating sequence characteristic and external factors (including weather factors and time-of-use price) in the prediction model framework. However, the average weather parameters cannot reflect the real weather conditions of all DEHSs owing to their wide geographical distributions. Some adjacent DEHSs are with same weather parameters, which can be used together in one LSTM to enhance the behavior influenced by the real weather conditions, and correct the contributions of average weather parameters.

In this paper, with the idea of trajectory prediction for autonomous driving in [30], we develop a C-LSTM model to predict the consumptions of DEHSs. The correlation of neighbor DEHSs is considered in this model to enhance the prediction accuracy. The block diagram of the electric power prediction of DEHS with the C-LSTM is shown in Fig. 8. This diagram illustrates the flow of a time series with some features of length S through two C-LSTM layers. However, the other impact factors can also be considered in this framework according to the requirement. In this diagram, h denotes the output (also known as the hidden state) and c denotes the cell state.

We extend a single LSTM cell into a C-LSTM network including multiple LSTM cells to processes the inputs separately and learn the interaction among the DEHSs. For the C-LSTM at time t:

$$\begin{cases} \left[\boldsymbol{W}_{ea,t}, P_{ri,t}, P_t^{n-1}, P_t^n, P_t^{n+1}\right] = x_t^k \\ c_t^{n-1}, h_t^{n-1} = LSTM^{n-1}\left(\left[\boldsymbol{W}_{ea,t}, P_{ri,t}, P_t^{n-1}, P_t^n\right], c_{t-1}^{n-1}, h_{t-1}^{n-1} \middle| \boldsymbol{W}^{n-1}\right) \\ c_t^n, h_t^n = LSTM^n\left(\left[\boldsymbol{W}_{ea,t}, P_{ri,t}, P_t^{n-1}, P_t^n, P_t^{n+1}\right], c_{t-1}^n, h_{t-1}^n \middle| \boldsymbol{W}^n\right) \\ c_t^{n+1}, h_t^{n+1} = LSTM^{n+1}\left(\left[\boldsymbol{W}_{ea,t}, P_{ri,t}, P_t^n, P_t^{n+1}\right], c_{t-1}^{n+1}, h_{t-1}^{n+1} \middle| \boldsymbol{W}^{n+1}\right) \end{cases}, \tag{13}$$

where $\boldsymbol{W}_{ea,t}$ is the weather parameters, $P_{ri,t}$ is the time-of-use price, P_t is the power consumption, superscripts n-1, n, n+1 represent the target DEHS, LSTM($\cdot$) is the state updating of the LSTM cells (i.e., short for (12)), $[\cdot,\cdot]$ means concatenating several vectors into one vector, and $\boldsymbol{W}$ is the trainable weights of LSTM.

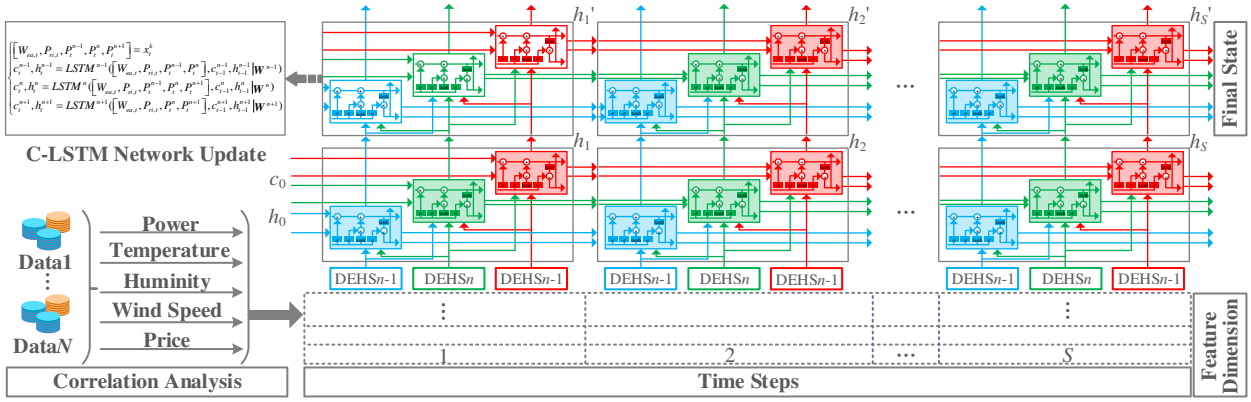

Fig. 8. Block diagram of electric power prediction of DEHS with C-LSTM.

Each DEHS is modeled by an LSTM cell, whose state recurrence is described as (12). The number of input arrows in the figure is the same as the number of input vectors in $[\cdot,\cdot]$ in the equations, which depends on the number of neighbor DEHSs. All three DEHS models are in the same types of inputs, outputs and LSTM cells, except for the different lengths of input. Each of the three LSTM cells is different from each other in the input size and trainable weights. In this framework, the number of DEHSs is not limited to three. More neighbor DEHSs can be added.

B. *Objective Function*

A day-ahead combined electricity and heat dispatch model for reducing wind power curtailment is established. Factors such as the fuel cost of CHP with TES, TPP, average operation and maintenance cost of EES, the cost of wind power curtailment and DEHS dispatch are considered. Summing up Eqs. (3), (5), (7), (9) and (10), the objective function of economic cost C_{EC} of day-ahead scheduling model is expressed in (14).

$$\min C_{EC} = C_{CT} + C_{TPP} + C_W + C_{EES} + C_{DEHS}. \quad (14)$$

C. Electric and Heating Networks Balance

(1) Electric network balance

Total generations and electric loads must be balanced at each operation period as described in (15).

$$\sum_{i=1}^{I} P^{\mathrm{E}}_{CHP,t} + \sum_{k=1}^{K} P_{TPP,\mathrm{t}} + \sum_{r=1}^{R} P_{EESr,t} + \sum_{m=1}^{M} (P_{WPPm,t} - \Delta P_{WPPm,t}) = P^{\mathrm{E}}_{L,t} + \sum_{n}^{N} (P^{\mathrm{E}}_{DEHSn,t} + \Delta P^{\mathrm{E}}_{DEHSn,t}), \quad (15)$$

where $P^{\mathrm{E}}_{L,t}$ is load electric demand at time t.

(2) District heating network unbalance

Since the inertia of the heating network can maintain the temperatures, the unbalance between thermal power generation and demand can be within a limited range as shown in (16).

$$\chi_{\min} P^{\mathrm{T}}_{L,t} \le (\sum_{i=1}^{I} P^{\mathrm{T}}_{CHPi,t} + \sum_{j=1}^{J} P^{\mathrm{T}}_{TESj,t}) \le \chi_{\max} P^{\mathrm{T}}_{L,t}, \quad (16)$$

where $P^{\mathrm{T}}_{L,t}$ is the heat demand at time t. $\chi_{\min}$ and $\chi_{\max}$ are the lower and upper limited proportions of adjustment in the district heating network.

D. Distributed Heating Networks Models

The operation constraints of electric power $P^{\mathrm{E}}_{DEHS,t}$, adjustment power $\Delta P^{\mathrm{E}}_{DEHS,t}$, thermal power $P^{\mathrm{T}}_{DEHS,t}$ and capacity $S^{\mathrm{T}}_{DEHS,t}$ for N DHNs are shown in Fig. 12. Individual DHN unbalance is considered with $P^{\mathrm{T}}_{DEHS,t}$ and the thermal requirement of DHL $P^{\mathrm{T}}_{DHL,t}$ to meet the heat load demand. $\zeta_{N,\min}$ and $\zeta_{N,\max}$ are the lower and upper limited proportions of adjustment of DHL N.

E. Solution

In the dispatch model, if constraints of all DHNs are considered, the resolving difficulty of the solution will be increased largely. The constraints are related to the comfort of all DHLs. To decrease the resolving difficulty of the solution, we propose to classify DHNs as different categories according to the thermal requirement level, capacity and location of individual DEHS. Then equally proportional distribution method is used to distribute dispatch command to individual DEHS.

In this paper, we cluster the corresponding specific behavior characteristics of all DEHS consumers based on the K-means method. The clustering results of all DEHS consumers based on K-means are shown in Fig. 9. According to the behavior characteristics and thermal requirement level of DHLs, the clustering results of all DEHS consumers are classified as two categories by the Fine Gaussian SVM method. Category 1 is defined as when the thermal requirement is high and the storage capacity is less, the DEHS will consume electric power to generate more thermal energy in the peak-time region. The others are defined as category 2. Moreover, to avoid the influence of behavior characteristics in the valley-time region when the SVM method is used, only the clustering results in the peak-time (30-84 points) are used to classify. Fig. 10 and Fig. 11 show the two classified categories of the DEHS consumers. It can be seen that the DEHSs in category 1 show significant variations in the peak-time region. The DEHSs in category 2 have low values and almost remain constant.

Considering the different requirements of thermal loads, the load consumers need to be classified to meet the restrictions of the dispatch model. If only one restriction is applied, the consumers' thermal requirements cannot be satisfied. If lots of restrictions are used, the resolving difficulty of dispatch model will be increased. Therefore, we classify two categories to reduce the constraints of DEHSs according to the characteristics in the daytime of power curves. This approach is simple and effective. However, our approach is not limited to this classification. More categories can be made according to the geographical location and control mode, which need more information. The specific classification algorithm is shown as follows.

Algorithm: DEHS Classification Based on K-means and SVM

Input: history electric power data of all DEHS consumers
Output: classification results for all DEHS consumers' ID
for n=1:1:N //N consumers
  do k-means (history data of DEHS n, Cluster No. = 1);
end
construct matrix A (include N cluster curves);
delete the data of A in the valley-time price region;
if $fitness(A(n)) \rightarrow$ constant **or** $P^{\mathrm{E}}_{DEHS,n} < P^{\mathrm{E}}_{DEHS,n,nom} \times 10\%$
  define category 2;
else define category 1;
end
construct classification sample B;
train sample B based on **Fine Gaussian SVM**;
export classification model to classify A;
return classification ID

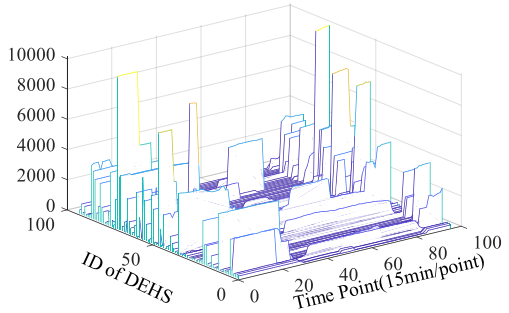

Fig. 9. Clustering results of DEHS consumers based on the K-means method.

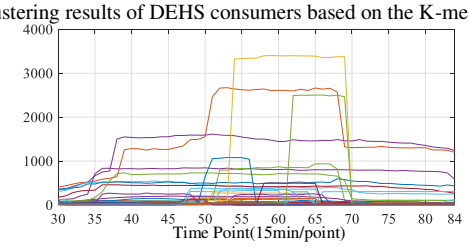

Fig. 10. Classification results of category 1.

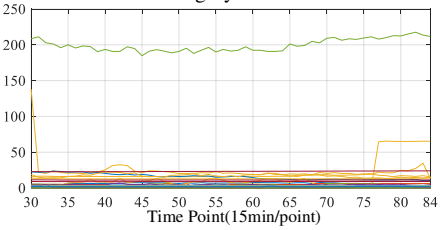

Fig. 11. Classification results of category 2.

Based on the above classification, two categories of DHNs

are obtained. Two sets of limited proportions of adjustment ($\varsigma_{c1,\min}$, $\varsigma_{c1,\max}$, $\varsigma_{c2,\min}$, and $\varsigma_{c2,\max}$) are used to meet the corresponding thermal requirements of two categories of DHNs respectively. The thermal constraints of two categories of DHNs $P^{\mathrm{T}}_{DEHSg,t}$ (g = 1, …, G is the number of Category 1) and $P^{\mathrm{T}}_{DEHSh,t}$ (h = 1, …, H is the number of Category 2) can be rewritten as in (17).

$$\begin{cases} \varsigma_{c1,\min}\sum_{g=1}^{G}P^{\mathrm{T}}_{DHLg,t} \le \sum_{g=1}^{G}P^{\mathrm{T}}_{DEHSg,t} \le \varsigma_{c1,\max}\sum_{g=1}^{G}P^{\mathrm{T}}_{DHLg,t} \\ \varsigma_{c2,\min}\sum_{h=1}^{H}P^{\mathrm{T}}_{DHLh,t} \le \sum_{h=1}^{H}P^{\mathrm{T}}_{DEHSh,t} \le \varsigma_{c2,\max}\sum_{h=1}^{H}P^{\mathrm{T}}_{DHLh,t} \end{cases} . \quad (17)$$

Then the optimal dispatch problem can be converted into a nonlinear quadratic programming problem. The Sequential Least Squares Programming method is used as a resolving solution in *Python*. The overall flow chart of the proposed framework of optimal dispatch based on prediction of DEHS with C-LSTM is shown in Fig. 12.

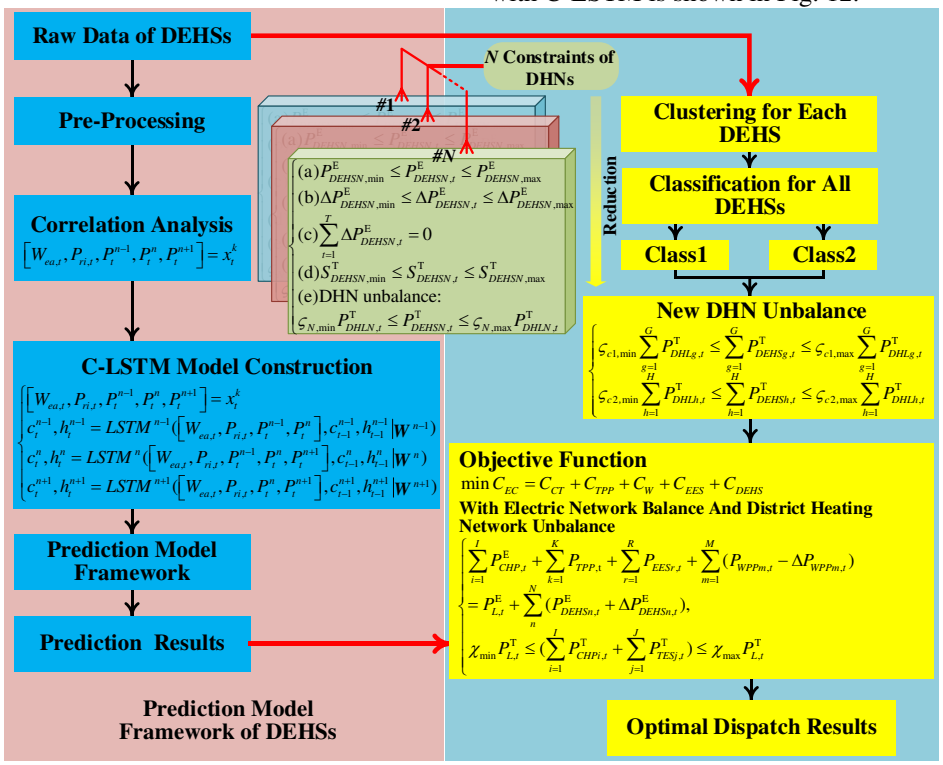

Fig. 12. The overall flow chart of the proposed framework of optimal dispatch based on prediction of DEHS with C-LSTM.

V. Case Study

To verify the effectiveness of the proposed prediction method and the optimal dispatch solution, numerous cases are conducted with real data in Liaoning provincial grid of China. It should be mentioned that the proposed method and the optimal dispatch solution can be applied in any system globally although the data used to validate the effectiveness is only from one country.

A. Prediction Method Validation

The proposed C-LSTM model is compared with two advanced methods: RNN and SVM. The C-LSTM model's fitness of train data and text data of DEHS is obtained by mean absolute error (MAE) loss function as shown in Fig. 13.

TABLE II
The Values of MAPE, RMSE and NRMSE of the Prediction Results With Different Prediction Methods

Prediction methods	MAPE	RMSE	NRMSE
SVM	1.298	4131	0.071
RNN	0.77	4013	0.069
C-LSTM	0.289	3881	0.068

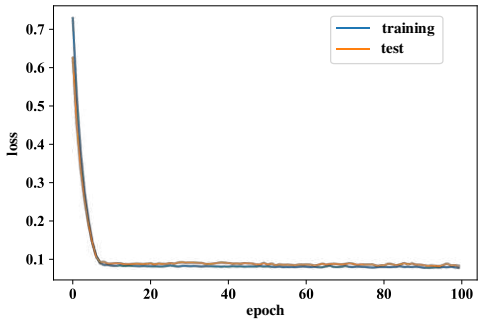

Fig. 13. The fitness of the training data and test data of DEHS.

In Fig. 13, with the increasing epoch, the losses gradually decrease below 0.1. The train and test sets are consistent, which proves the high accuracy of the C-LSTM model. The prediction results with different methods are shown in Fig. 14 and Table II.

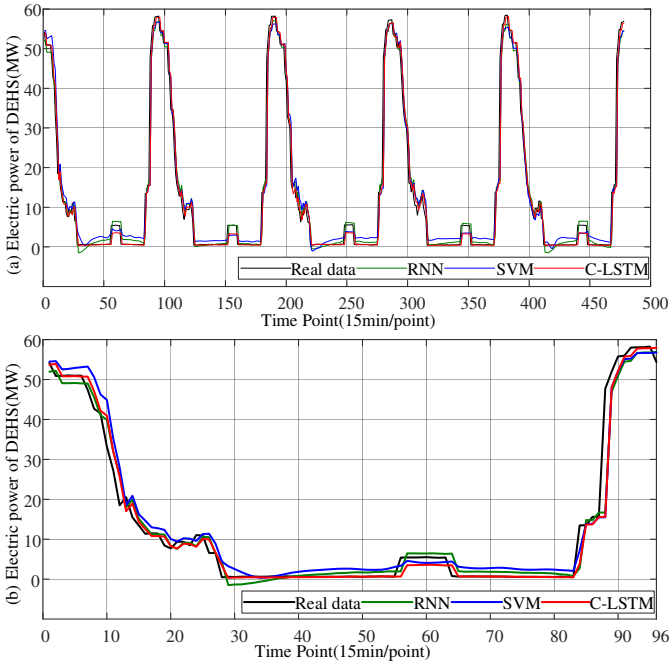

Fig. 14. Real data and prediction data of DEHS. (a) The real data and prediction data for five days; (b) The real data and prediction data for the first day.

In Fig. 14(a), with different methods, the overall prediction trends are consistent considering the weather and time-of-use price. Fig 14(b) shows that the prediction result with C-LSTM is closest to the real data. In Table II, it can be seen that MAPE, root mean square error (RMSE) and normalized root mean square error (NRMSE) with C-LSTM are the least, which shows the higher accuracy of the proposed model.

B. Optimal Dispatch Validation

The key point of the optimal dispatch is the effectiveness of dispatching DEHS with the respect of the day-ahead optimal dispatch. Thus, two methods (with DEHS and without DEHS) are compared. Electric and heat load power curves are predicted. The Fig. 15 shows wind power curves of a month (30 days). The wind data is given in every 15 mins. The two selected curves have the maximum and minimum output power in the month. It can prove that the proposed methods can copy with different operating conditions. In Case 1, the lower wind power curve is applied, and the upper wind power curve is used in Case 2. The electric power curves of two categories of DEHS1 and DEHS2 are predicted based on the proposed C-LSTM model. The simulation parameters are the same with the Liaoning provincial grid as shown in Table III.

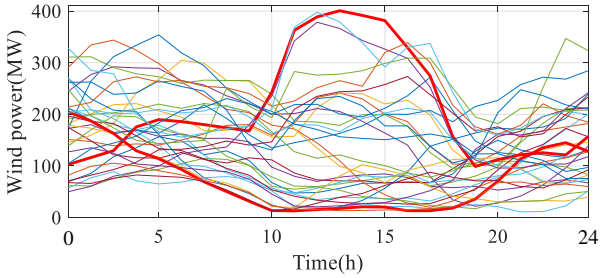

Fig. 15. Typical wind power curves.

The optimization results of the two cases with different methods are shown in Figs. 16 and 17. In Fig. 16(a), the electric

TABLE III
SIMULATION PARAMETERS

Parameters	Values	Parameters	Values
c_v	0.15	c_{o2}	26 USD/MW
a_i	0.0044 USD/MW^2	c_{o3}	10 USD/MW
b_i	13.29 USD/MW	$\chi_{\min}$	0.9
c_i	39 USD	$\chi_{\max}$	1.1
c_{o1}	10 USD	$\varsigma_{c1,\min}$	0.9
a_k	0.03 USD/MW^2	$\varsigma_{c1,\max}$	1.1
b_k	23.66 USD/MW^2	$\varsigma_{c2,\min}$	0.8
c_k	16.22 USD	$\varsigma_{c2,\max}$	1.2
c_Q	30 USD/MW	N	94

power of load (P_L^E) is supplied by power sources in the electric network. With the two methods, the electric power of CHP P_{CHP}^E and TPP P_{TPP} are generally consistent. The proportion of electric power of ESS P_{ESS} in the grid is relatively less. In this case, the wind power curtailment cannot be reduced by EES only. The wind power consumption P_{WPP} with the proposed dispatching DEHS is more than that without the DEHS.

In the peak-time region (from time points 36 to 90), the wind power output is so high, that the outputs of CHP, TPP and EES are close to their upper limits. In Fig. 16(b), around the time point 12, due to the decrease of the electric power of load, the wind power is curtailed to balance the electric power. Thanks to the proposed dispatching DEHS, the consumptions of DEHS1 and DEHS2 are shifted to reduce the wind power curtailment. It can be seen that the peak wind power curtailment is reduced by about 30 MW (i.e., 30%). The lifetime of the EES may be reduced.

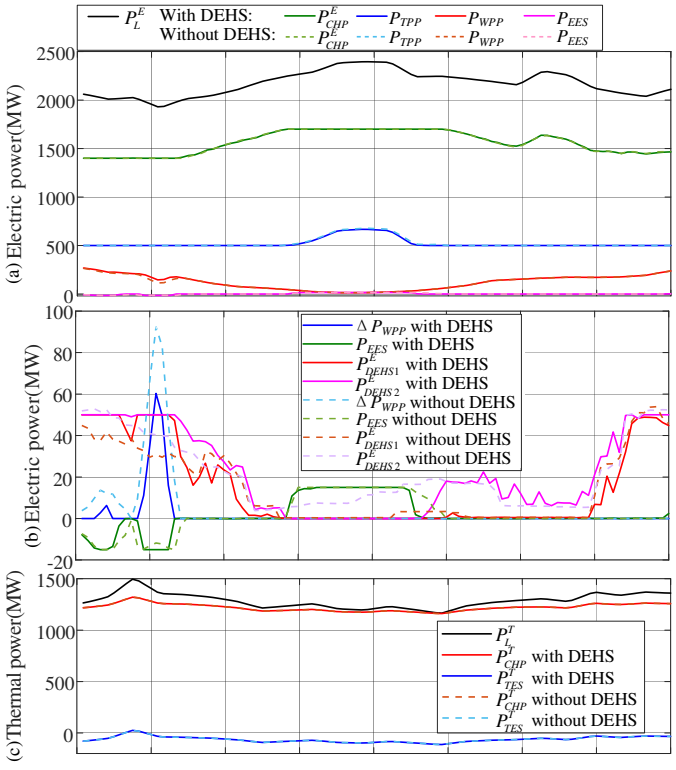

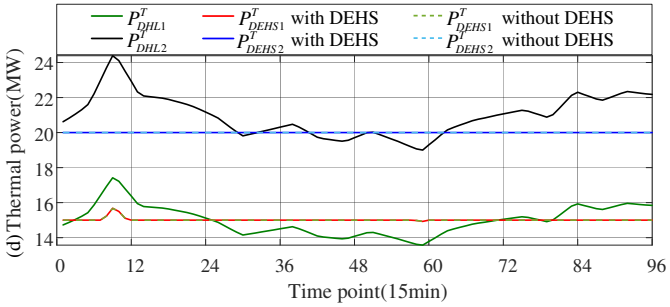

Fig. 16. The dispatch results in Case 1. (a) Electric power of load, CHP, WPP and EES; (b) Electric power of wind power curtailment, ESS, DEHS1 and DEHS2; (c) Thermal power in district heating network; (d) Thermal power in DHNs.

Figs. 16(c) and (d) show the thermal supply and consumption in the district and distributed heating networks, respectively. It can be seen that, in the district heating network, due to the help of TES, the requirement of thermal power with two methods can be met for the residents. In the distributed heating networks, the thermal requirement level of DEHS1 is stricter than DEHS2, and the requirements are met. The final economic costs of the dispatch model C_{EC} are 5,479,070 USD and 5,497,769 USD with DEHS and without DEHS, respectively. The results of Case 2 are shown in Fig. 17.

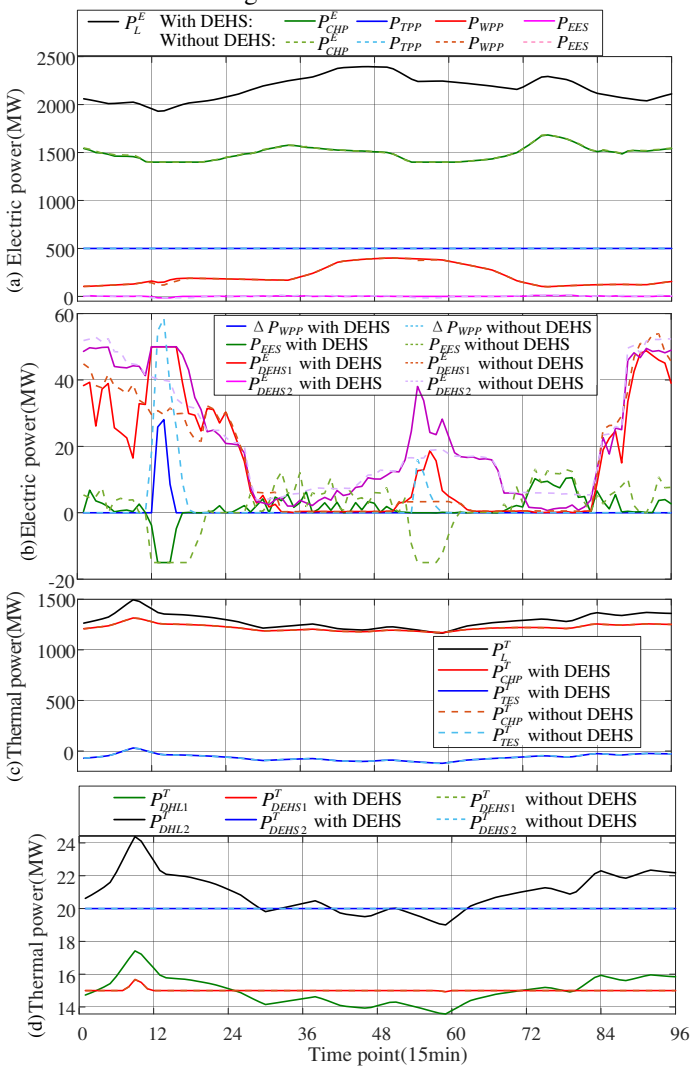

Fig. 17. The dispatch results in Case 2. (a) Electric power of load, CHP, WPP and EES; (b) Electric power of wind power curtailment, ESS, DEHS1 and DEHS2; (c) Thermal power in Thermal power in district heating network; (d) Thermal power in DHNs.

In Fig. 17(a), the wind power is higher than that in Fig. 16(a). In the peak-time region, there is a small change in the outputs of the CHP and TPP. It is because that the wind power output is large and its trend is similar to electric load. With dispatching DEHS, wind power consumption is larger than that without DEHS. As shown in Fig. 17(b), thanks to the adjustment of the consumption of DEHS1 and DEHS2, nearly 30 MW (i.e., 50%) of the peak wind power curtailment is reduced. It can be seen from Figs. 17(c) and (d), the thermal supply can meet the thermal requirement in the district and distributed heating networks respectively. The final economic costs C_{EC} are 5,142,018 USD and 5,157,416 USD with DEHS and without DEHS, respectively. Therefore, the proposed dispatch method can reduce wind power curtailment and economic costs.

VI. Conclusion

This paper proposes a framework of optimal dispatch based on the prediction model with the correlation-based long short-term memory of distributed electric heating storage. The prediction model, considering their behavior characteristics including weather and time-of-use price, improves the prediction accuracy of distributed electric heating storage. The effectiveness of the proposed prediction model and the dispatch method are verified through simulations. Compared with the state-of-the-art techniques of support vector machine and recurrent neural networks, the mean absolute percentage error with the proposed correlation-based long short-term memory can be reduced by 1.009 and 0.481 respectively. Compared with conventional method, the peak wind power curtailment with dispatching distributed electric heating storage is reduced nearly 30% and 50% in two cases respectively.

Acknowledgments

This work was supported in part by the China Postdoctoral Science Foundation under Grant 2019M651144, in part by the Liaoning Provincial Department of Education Research Funding under Grant LQGD2019005.

References

[1] Y. Dai, L. Chen, Y. Min, Q. Chen, K. Hu, J. Hao *et al*., "Dispatch model of combined heat and power plant considering heat transfer process," *IEEE Transactions on Sustainable Energy*, vol. 8, no. 3, pp. 1225-1236, 2017.

[2] Z. Yang, C. Gao and M. Zhao, "Coordination of integrated natural gas and electrical systems in day-ahead scheduling considering a novel flexible energy-use mechanism," *Energy Conversion and Management*, vol. 196, pp. 117–126, 2019.

[3] Y. Zhou, J. Wu and C. Long, "Evaluation of peer-to-peer energy sharing mechanisms based on a multiagent simulation framework," *Applied Energy*, vol. 222, pp. 993-1022, 2018.

[4] C. Wang, Y. Zhou, J. Wu, J. Wang, Y. Zhang and D. Wang, "Robust-index method for household load scheduling considering uncertainties of customer behavior," *IEEE Transactions on Smart Grid*, vol. 6, no. 4, pp. 1806-1818, 2015.

[5] C. Wang, Y. Zhou, B. Jiao, Y. Wang, W. Liu and D. Wang, "Robust optimization for load scheduling of a smart home with photovoltaic system," *Energy Conversion and Management*, vol. 102, pp. 247-257, 2015.

[6] M. Song, C. Gao, H. Yan and J. Yang, "Thermal battery modeling of inverter air conditioning for demand response," *IEEE Transactions on Smart Grid*, vol. 9, no. 6, pp. 5522-5534, 2018.

[7] Q. Chen, N. Liu, C. Hu, L. Wang and J. Zhang, "Autonomous energy management strategy for solid-state transformer to integrate PV-assisted EV charging station participating in ancillary service," *IEEE Transactions on Industrial Informatics*, vol. 13, no. 1, pp. 258-269, 2017.

[8] Y. Dai, L. Chen, Y. Min, P. Mancarella, Q. Chen, J. Hao *et al*., "Integrated dispatch model for combined heat and power plant with phase-change thermal energy storage considering heat transfer process," *IEEE Transactions on Sustainable Energy*, vol. 9, no. 3, pp. 1234-1243, 2018.

[9] C. Wu, W. Gu, P. Jiang, Z. Li, H. Cai and B. Li, "Combined economic dispatch considering the time-delay of district heating network and multi-regional indoor temperature control," *IEEE Transactions on Sustainable Energy*, vol. 9, no. 1, pp. 118-127, 2018.

[10] B. Liu, K. Meng, Z. Y. Dong and W. Wei, "Optimal dispatch of coupled electricity and heat system with independent thermal energy storage," *IEEE Transactions on Power Systems*, vol. 34, no. 4, pp. 3250-3263, 2019.

[11] P. S. Sauter, B. V. Solanki, C. A. Cañizares, K. Bhattacharya and S. Hohmann, "Electric thermal storage system impact on northern communities' microgrids," *IEEE Transactions on Smart Grid*, vol. 10, no. 1, pp. 852-863, 2019.

[12] S. Wong and J. Pinard, "Opportunities for smart electric thermal storage on electric grids with renewable energy," *IEEE Transactions on Smart Grid*, vol. 8, no. 2, pp. 1014-1022, 2017.

[13] F. Wei *et al*., "A novel thermal energy storage system in smart building based on phase change material," *IEEE Transactions on Smart Grid*, vol. 10, no. 3, pp. 2846-2857, 2019.

[14] Y. Zhou, C. Wang, J. Wu, J. Wang, M. Cheng and G. Li, "Optimal scheduling of aggregated thermostatically controlled loads with renewable generation in the intraday electricity market," *Applied Energy*, vol. 188, pp. 456-465, 2017.

[15] J. Yu, X. Shen and H. Sun, "Economic dispatch for regional integrated energy system with district heating network under stochastic demand," *IEEE Access*, vol. 7, pp. 46659-46667, 2019.

[16] M. Cui, M. Khodayar, C. Chen, X. Wang, Y. Zhang and M. E. Khodayar, "Deep learning based time-varying parameter identification for system-wide load modeling," *IEEE Transactions on Smart Grid*, 2019, Early Access.

[17] C. Zheng, S. Wang, Y. Liu, C. Liu, W. Xie, C. Fang *et al*., "A novel equivalent model of active distribution networks based on LSTM," *IEEE Transactions on Neural Networks and Learning Systems*, vol. 30, no. 9, pp. 2611-2624, 2019.

[18] W. Lin, G. Wu, X. Wang and K. Li, "An artificial neural network approach to power consumption model construction for servers in cloud data centers," *IEEE Transactions on Sustainable Computing*, 2019, Early Access.

[19] M. Dong and L. S. Grumbach, "A hybrid distribution feeder long-term load forecasting method based on sequence prediction," *IEEE Transactions on Smart Grid*, 2019, Early Access.

[20] J. Schmidhuber, "Deep learning in neural networks: an overview," *Neural Networks*, vol. 61, pp. 85-117, 2015.

[21] M. Afrasiabi, M. Mohammadi, M. Rastegar and A. Kargarian, "Multi-agent microgrid energy management based on deep learning forecaster," *Energy*, 2019, Early Access.

[22] S. A. Seshia, S. Hu, W. Li and Q. Zhu, "Design automation of cyber-physical systems: challenges, advances, and opportunities," *IEEE Transactions on Computer-Aided Design of Integrated Circuits and Systems*, vol. 36, no. 9, pp. 1421-1434, 2017.

[23] Y. Liu, S. Hu, H. Huang, R. Ranjan, A. Y. Zomaya and L. Wang, "Game-theoretic market-driven smart home scheduling considering energy balancing," *IEEE Systems Journal*, vol. 11, no. 2, pp. 910-921, 2017.

[24] S. Wen, Y. Wang, Y. Tang, Y. Xu, P. Li and T. Zhao, "Real-time identification of power fluctuations based on LSTM recurrent neural network: A case study on Singapore power system," *IEEE Transactions on Industrial Informatics*, vol. 15, no. 9, pp. 5266-5275, 2019.

[25] C. Lai, W. Chien, L. T. Yang and W. Qiang, "LSTM and edge computing for big data feature recognition of industrial electrical equipment," *IEEE Transactions on Industrial Informatics*, vol. 15, no. 4, pp. 2469-2477, 2019.

[26] W. Kong, Z. Y. Dong, Y. Jia, D. J. Hill, Y. Xu and Y. Zhang, "Short-term residential load forecasting based on LSTM recurrent neural network," *IEEE Transactions on Smart Grid*, vol. 10, no. 1, pp. 841-851, 2019.

[27] J. Toubeau, J. Bottieau, F. Vallée and Z. De Grève, "Deep learning-based multivariate probabilistic forecasting for short-term scheduling in power markets," *IEEE Transactions on Power Systems*, vol. 34, no. 2, pp. 1203-1215, 2019.

[28] C. M. Correa-Posada and P. Sánchez-Martín, "Integrated power and natural gas model for energy adequacy in short-term operation," *IEEE Transactions on Power Systems*, vol. 30, no. 6, pp. 3347-3355, 2015.

[29] Y. Zhao, L. Ye, Z. Li, X. Song, Y. Lang, J. Su. "A novel bidirectional mechanism based on time series model for wind power forecasting," *Applied Energy*, vol. 177, pp. 793-803, 2016.

[30] L. Hou, L. Xin, S. E. Li, B. Cheng and W. Wang, "Interactive trajectory prediction of surrounding road users for autonomous driving using structural-LSTM network," *IEEE Transactions on Intelligent Transportation Systems*, 2019, Early Access.